# Digital Twin For Electric Vehicle Monitoring

Luca Cavanini, Pawel Majecki, Mike J. Grimble, Alan Devine and Curt Hillier

*Abstract*— **This paper considers the results of a study that investigated the use of Digital Twin technologies for Electric Vehicle propulsion system state of health monitoring. Modern vehicles can share large amounts of data in the cloud through wireless connections. Digital twins represent an effective approach to exploit data-sharing and modern data-driven Artificial Intelligence and Machine Learning technologies, including vehicle monitoring or driving scenarios analysis. This study describes the design and development of a proof-of-concept digital twin demonstrator, that can detect fault/fault-free conditions in electric motor components. It can be used to assess the overall electric drive Failure Rate and to estimate the Remaining Useful Lifetime of the motor. The demonstrator developed within a simulation environment has been validated over a wide set of simulated operating scenarios demonstrating the effectiveness of the proposed approach.**

*Keywords*—**Digital Twin, Electric Vehicle, Electric Motor, Artificial Intelligence.**

## I. Introduction

Digital Twin (DT) technology was defined in 2012 by the National Aeronautics and Space Agency (NASA). It is a virtual representation of a production system that can run on different simulation systems that is characterized by the synchronization between the virtual and a real system. This is thanks to sensed data and connected smart devices, mathematical models, and real-time data elaboration [1]. A DT is composed as follows:

- A real-world physical system continuously monitored by sensors and software,
- A virtual system reflecting real system behaviour, designed using data-driven and model-based techniques and updated by shared data, and a data flow that ties virtual and physical systems in the real and virtual operating spaces. This allows continuous updating of the virtual plant model according to the real plant system measurements [2].

In recent years, several DT-based approaches have been studied and proposed for automotive applications including intelligence driver assistance, autonomous navigation, Electric Vehicle (EV) health monitoring, or battery management systems integration [2].

A DT demonstrator for EV automotive applications is described in the following. The system demonstrates the capabilities of DT technologies for monitoring the state of health of modern EV Electric Motors (EMs) [3]. The DT is exploited to detect a set of faults in four EMs of the EV, one for each wheel [4]. The faults considered affect the EM speed sensor, the EM internal insulation and related changes in the motor temperature dynamics, and the EM bearing system with related vibration dynamics [5]. Each fault has been modelled using well-known model-based and data-driven modelling methods. The mismatch between the DT virtual model and the real-world system data was captured and used to detect fault and fault-free operating conditions representing the different components of each motor. The analysis of real-world model data and virtual model signals was performed by exploiting the abilities of modern data-driven fault detection algorithms.

The data-driven fault detection algorithm output signals were used to provide feedback to the user about the status of the health of each EM and related subsystems. The fault detection system has been integrated with a Remaining Useful Life (RUL) [6] and Failure Rate (FR) [7] estimation module, to evaluate the loss of RUL and detect the possibility that a failure is likely on a particular EM. The demonstrator has been validated by testing it while activating/deactivating different faults on different EMs. This was over a long-horizon simulation scenarios, with vehicle velocities obtained from driving cycles (FTP75, US06, WLTP and NEDC) [8].

The paper is structured as follows. Section II describes the DT demonstrator, Section III presents the models of vehicle and Energy Management System (EMS), Section IV presents the data analytics module based on data-driven ML fault detection and health monitoring algorithms. Section V reports test results, and Section VI concludes the paper.

## II. Digital Twin Demonstrator

In this section, the DT demonstrator system is presented. The logical architecture of the system to be emulated is shown in Figure 1. The Fault Control Interface is used to activate/deactivate faults affecting EMs on the Real-World Model of the EV. This interface is composed of a set of switches that change the internal structure of the Real-World Model so that each EM subsystem can be affected by one of the faults.

Data measured from the Real-World Model are passed to the Cloud by a Data Flow transmission system that connects the

Luca Cavanini is with Industrial Systems and Control Ltd, Glasgow, UK (e-mail: l.cavanini@isc-ltd.com) and Università Politecnica delle Marche, Ancona, Italy (corresponding author, phone: 0039-071-2204314; fax: 0039-071-2204315; e-mail: l.cavanini@univpm.it).

Pawel Majecki and Mike J. Grimble are with with Industrial Systems and Control Ltd, Glasgow, UK (e-mail: {pawel, m.grimble}@isc-ltd.com). Mike J. Grimble is also with University of Strathclyde, Glasgow, UK (e-mail: m.grimble@isc-ltd.com).

Alan Devine is with NXP Semiconductors, East Kilbride, UK (e-mail: alan.devine@nxp.com).

Curt Hillier is with NXP Semiconductors, Austin, USA (e-mail: curt.hillier@nxp.com).

virtual and real environments. The Virtual World EM Models generate simulated data to be compared with the Real-World Model measured data.

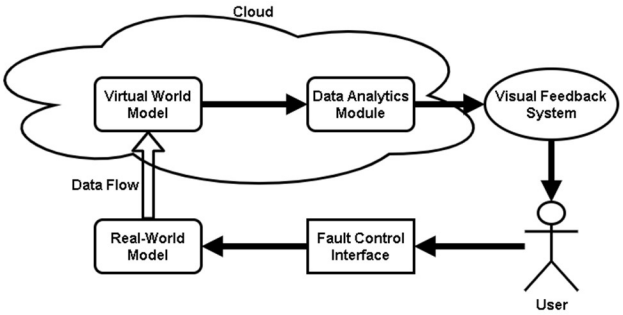


Fig. 1. Logical Digital Twin Architecture.

These real and virtual signals are analyzed by a Data Analytics Module that exploits Machine Learning (ML) and data-driven Artificial Intelligence (AI) capabilities to analyze features to detect faults within each EM. Furthermore, this module estimates RUL and FR that represent the state of the health of each motor. The results are presented to the user through the Visual Feedback System.

## III. Electric Motor Model

In this section, the simulation models considered for developing the real, and virtual EV models are presented. The EV is assumed to be characterized by four independent EMs and each EM has been represented by the closed-loop electromechanical dynamics of the motor. Furthermore, each EM includes subsystems representing the EM speed sensors, the EM temperature dynamics, and vibrations. Faults can be activated or deactivated on these different subsystems.

### A. EM Closed-Loop Dynamics

For this example, the EM was a Permanent Magnet Synchronous Motor (PMSM) [9]. The closed-loop model of the motor was represented using a model-based control approach exploiting the Clark and Park transform methods, and a Field Oriented Control (FOC) approach [10]. The closed loop dynamics of the EM includes a set of Proportional Integral (PID) controllers. For a description of the PMSM modelling and FOC methods the reader is referred to [11]. In the approach, the variables to interface the controlled PMSM with the rest of the DT-based system are the reference motor speed $\omega_r$ [rpm]. This is computed from the vehicle reference speed, and the measured speed of the $i$-th EM $\omega_i$[rpm] with $i \in \{1,2,3,4\}$ which drives the different EM subsystems dynamics presented in the following sections.

### B. EM Sensor Speed Model

Each EM has a velocity sensor to measure the rotational speed $\omega_i$[rpm]. The EM model to emulate the virtual DT is not affected by any noise or disturbance. On the other hand, the real-world model of the EM speed sensor contains the effects of noise and faults [12]. It is modelled by introducing a white noise additive signal $n_{s,i}(t)$ on the speed $\omega_{m,i}$ measured from the sensor, whereas the fault is modelled as a constant offset signal $f_\omega(t) = 15$ [rpm], so that:

$$\omega_{m,i}(t) = \omega_i(t) + n_{s,i}(t) + f_\omega(t) \quad (1)$$

In the case of the DT virtual model $\omega_{m,i}(t) = \omega_i(t)$.

### C. EM Temperature Model

Changes in EM temperature dynamics represent the effects of an EM internal insulation system faults or loss of performance of the EM colling system. To develop an EM temperature model to represent the fault and fault-free operating conditions, a model of motor heating dynamics has been found from analysis of the dataset from Paderborn University [13] and collecting data in both normal and faulty operating conditions. By using a black-box system identification method [14], a discrete-time state-space model has been identified in the form:

$$\dot{x}(t) = Ax(t) + Bu(t) \quad (2)$$
$$y(t) = Cx(t) + Du(t) \quad (3)$$

where $y = T_i$ [C] is the $i$-th EM temperature, $u = \omega_i$ [rpm] is the related motor output speed, $x \in \mathbb{R}^{n_x}$ is the state-space model state vector. The state-space matrices are:

$$(A, B, C, D) \in \{(A_f, B_f, C_f, D_f), (A_c, B_c, C_c, D_c)\} \quad (4)$$

where $(A_f, B_f, C_f, D_f)$ are matrices describing the EM in temperature faulty conditions and $(A_c, B_c, C_c, D_c)$ are matrices relating to fault-free operating conditions. The real-world EM model also has an additive white noise $n_{T_i}(t)$ signal affecting the measured temperature (that is neglected in the DT virtual world model) such that

$$y(t) = T_i(t) = Cx(t) + Du(t) + n_{T_i}(t). \quad (5)$$

### D. EM Vibration Model

Vibrations are defined as changes in the acceleration $a_i(t)$ over the direction normal to the surface of the $i$-th EM stator. Each EM is characterized by a certain vibration frequency spectrum related to the corresponding EM rotational speed. Changes in the spectrum would reflect a fault affecting the EM components e.g., damaged bearings. Modelling dynamics of EM vibration is a complex task that in the proposed approach has involved an identification procedure like the method used for modelling the EM temperature dynamics. In the proposed approach, a dataset from the Case Western Reserve University [15] has been considered. This dataset contains both fault-free and faulty data relating to bearing damage conditions. By switching models' coefficients using the fault activation command signals, the bearing fault is activated/deactivated in the $i$-th EM.

### E. Comparison of Faulty and Fault-Free Conditions

The comparison of EMs subsystems behavior in fault and fault-free conditions is shown in Figure 2. The plots include: the fault and noise free virtual system outputs (blue lines), the real system fault-free outputs (dotted red lines) and the real system faulty outputs (dashed yellow lines). These signals are typical examples of the type of signals to be evaluated by the data analytics module to detect the various faults affecting the EMs and related subsystems.

## IV. Electric Motor Model

In this section, the data analytics module is presented. The module is logically composed of two subsystems: (1) fault detection system that detects faults occurring on the *i*-th EM; (2) the State of Health (SoH) monitoring system that estimates RUL and FR percentage of the *i*-th EM. Furthermore, a discussion of the data transmission flow connecting the real-world vehicle to the cloud is provided.

### *A. Data Analytics Module: Fault Detection System*

The fault detection system is composed of a set of fault detection modules to detect different faults associated with each EM. In the proposed approach, three fault detection modules were developed to detect the bearing, sensor speed and temperature faults. These modules have been structured as shown in Figure 3. Data measured from the real-world model and obtained from the DT virtual model are compared by a data-driven ML algorithm that generates features $f_{i,j}(k)$. The 'features' are signals that have no physical meaning and indicate if (based on the analysed samples) the *j*-th fault affects the *i*-th EM. The features therefore can assume two values, corresponding to the estimated faulty $\left(f_{i,j}(k) = 0\right)$ or fault-free $\left(f_{i,j}(k) = 1\right)$ conditions. The evaluated features are collected within a buffer of a length defined during the DT-based system setup. The averaged values of the features collected within the buffer are then computed and compared against a predefined threshold value, resulting in the final 'fault-free' vs 'faulty' estimate.

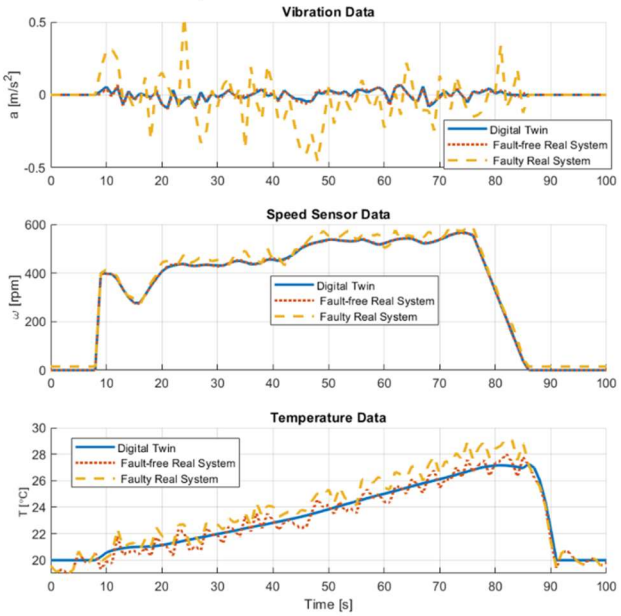


Fig. 2. Comparison of EM signals in Faulty and Fault-free conditions with respect to the DT virtual model.

The data-driven fault extraction algorithm was developed by using Supervised Learning methods. In particular, the speed sensor and vibration fault features were generated by analysing the data using Neural Networks (NNs) [16] trained to provide an output feature value $f_{i,j}(k) \in \{0,1\}$. On the other hand, the temperature fault features were generated by comparing samples given from the real-world and DT systems using a Support Vector Classifier (SVC) [17] computing the output feature signal $f_{i,j}(k) \in \{0,1\}$. The NNs and SVC algorithms are presented briefly in the following together with some details about the training phase.

***Neural Network.*** An artificial NN is a computational model inspired by the human brain structure, that can learn and replicate nonlinear behaviour from analysis of available data used during the training phase [18]. The NN is composed of three layers of Radial Basis Function neurons with 2 neurons in the input layer, 25 neurons in the hidden layer and 1 output layer neuron. The NN has been trained with a dataset of real-world system measured data and DT virtual model signals, and the related labels indicating the fault-free and faulty operating conditions were also provided. The NN training was performed using the back-propagation algorithm to calibrate network hyperparameters. The training validation performance was quantified as 80% of correctly classified samples for the speed sensor fault NN and 75% for the vibration fault NN.

***Support Vector Classifier:*** A SVC has been selected to detect temperature fault features. For this problem, this approach is more suitable due to the intrinsic classification-oriented nature of Support Vector-based policies and provides more degrees of freedom in the algorithm design. It acts directly on the internal structure of the ML-algorithm and formulates the identification problem in the most suitable form [19]. In the classification theory, support Vector-based methods can be used to find the maximum separating margin for a linearly separable dataset by mapping samples to a hyperspace defined according to the available data [20]. The distance between all these points and the line is the maximum possible among all possible decision boundaries, making it optimal. In the proposed approach, the labelled temperature data obtained from the real-world model and from the DT system are used to train the SVC that is then used to detect features corresponding to the related fault. The validation results achieved by the trained SVC indicate 83% fault detection performance.

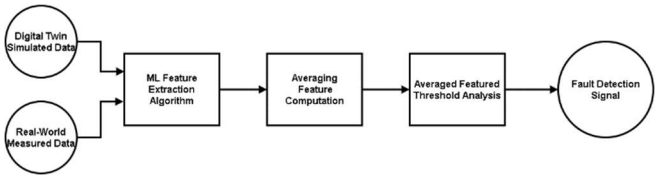


Fig. 3. DT-based fault detection algorithm structure.

***Machine Learning Feature Extraction System Training.*** To develop the SVC and NN feature extraction systems, the data were first separated into the training, testing and validation subsets. Each of these datasets is composed of a set of input signals (measurements from DT and the real-world system) and the related labels indicating a fault or fault-free condition in the real-world vehicle system. The ML methods were then trained to approximate the mapping between the input data

and the output labels. Recall that the features generated by the ML methods are variables belonging to the set [0,1]. By averaging the values of the features collected in a buffer (of predefined length), the averaged buffer value can be computed and compared with the threshold value (a user-defined parameter). When the average buffer value is higher than the threshold value, the system is considered in fault free conditions, whereas if the value is lower than the threshold the system concludes it is a faulty condition. The value of the threshold is selected by the designer according to the dynamics of the subsystem, the fault, and the averaged value of the buffer and related size. Because of the different aspects representing the averaged featured value dynamics, the threshold value, as for the buffer size and other parameters represents a tuning parameter to be adjusted during the software setup phase.

More specifically, the extracted features $f_{i,j}(k)$ are averaged within buffers $b_{i,j} \in \mathbb{R}^{N_{b_{i,j}}}$ of dimensions $N_{b_{i,j}}$, with $i \in \{1,2,3,4\}$ indicate the *i*-th EM and $j \in \{1,2,3\}$ refers to the *j*-th fault (e.g., $j = 1$ indicates the *i*-th EM speed sensor fault). The values stored within the buffer are iteratively updated according to a First-In Last-Out (FILO) approach, and only if the measured vehicle speed is positive, i.e., only if the vehicle is moving. The averaged value of the buffer $b_{i,j}(k)$, indicated by $\bar{f}_{i,j}(k)$, is then iteratively computed and compared with the threshold $\bar{f}_{i,j}^{th}$ such that

$$\bar{f}_{i,j}^{Alarm}(k) = \begin{cases} 1 & if \ \ \bar{f}_{i,j}(k) \geq \bar{f}_{i,j}^{th} \\ 0 & if \ \ \bar{f}_{i,j}(k) < \bar{f}_{i,j}^{th} \end{cases} \quad (6)$$

where $\bar{f}_{i,j}^{Alarm}(k)$ is the fault detection alarm set to 1 if a fault-free condition is detected and set to 0 in a faulty state. The value of the $\bar{f}_{i,j}^{Alarm}$ is then provided to the user, informing them about the state of each EM subsystem.

### B. Data Analytics Module: SOH Monitornig Systems

The fault alarm signals defined by the fault detection systems are also used to evaluate the Failure Rate and the Remaining Useful Lifetime (RUL) of the EM according to the detected conditions of the EM components. The FR provides an estimate of the failure rate due to different faults detected affecting the EM. The RUL gives an estimate of the remaining lifetime of the EM with respect to actual and past faults degrading the motor performances. In the proposed approach, the FR of the *i*-th EM is defined as

$$FR_i(t) = 100 \sum_{k=1}^{n_f} \bar{b}_{k,j}(k)\, \bar{F}_{k,j}^{Alarm}(k) \frac{1}{2N_{b_{k,j}}} \quad (7)$$

where $n_f$ is the number of faults considered in the analysis, the variable $\bar{F}_{k,j}^{Alarm}$ is defined according to the instantaneous value of the fault alarm signal $\bar{f}_{k,j}^{Alarm}(t)$ such that

$$\bar{F}_{k,j}^{Alarm}(t) = \begin{cases} 1 & if \ \ \bar{f}_{k,j}^{Alarm}(t) = 1 \\ 2 & if \ \ \bar{f}_{k,j}^{Alarm}(t) = 0 \end{cases} \quad (8)$$

and $\bar{b}_{k,j}(t)$ represent the sum of values of entries stored in the buffer $b_{k,j}(t)$ at the *t*-th time instant. The RUL of the *i*-th EM is estimated as the percentage of the nominal initial RUL such that

$$RUL_j(t) = 100 + \min\left(0, -\left(-\ln\left(\frac{\int \bar{F}_{k,j}^{Alarm}(t)dt}{t}\right)\right)^{-1}\right) \quad (9)$$

where the term $\left(-\ln\left(\frac{\int \bar{F}_{k,j}^{Alarm}(t)dt}{t}\right)\right)^{-1}$ represents the degradation function i.e., the loss of lifetime of the electric motor due to the detected faults. The nominal RUL is 100% and it is a decreasing monotonic function. This effectively considers the effect of the previous faults also in the case when those disappear and permits to estimate the RUL as a monotonically decreasing function.

### C. Data Flow Analysis

A key element of DT technology is the data transmission system needed to connect the real-world system to the cloud/edge environment where the DT model and data analytics algorithms reside. In modern automotive applications, EV could be fully connected, and large amounts of measured data could be transmitted. However, in practice, storing and sharing such data will usually be limited by the transmission bandwidth available. For this reason, the DT system should be designed assuming a limited data transmission rate. In the proposed approach, the DT-based system has been designed to operate with a transmission frequency of 1 Hz i.e., measured real-world data are transmitted to the cloud by sending only one sample of each measured signal at each second. The DT virtual model simulated with a sampling frequency of 10 Hz, whereas the data analytics algorithms are executed with a frequency of 1 Hz. Signals transmitted to the cloud are: the measured real vehicle speed, the measured EM temperature, vibration and speed, for a total of 13 samples transmitted every second. Assuming that each sample is represented by a floating-point variable requiring 4 bytes for its digital 32-bit representation, the amount of data transmitted at each sampling instant from the vehicle to the cloud is 52 Bytes. This is considered reasonable for this application. Note that in reality the data transmission rate will be higher once a transmission protocol with safety/security features is included.

The design of the transmission system and related sizing of the DT-based fault detection algorithm structure were performed considering the data transmission specifications. The system has been calibrated to provide feedback with a certain time-delay between the activation of the fault and related correct fault detection signal. The time-delay is related to the number of features collected and evaluated iteratively by the system. By increasing the data transmission speed, it is possible to increase the number of samples evaluated from the system at each iteration. Increasing the data transmission rate enables an increase in the number of samples evaluated, reducing the time interval required from the system to detect a fault. Changes in the data-transmission flow would need an adjustment of buffer size and related averaged buffer threshold values used to evaluate the faulty conditions. This modification would be customized for the different subsystems and the related faults considered from the DT system to reduce the time interval required to detect the

fault/fault-free conditions after the activation/deactivation of each fault.

## V. Simulation Results

In this section, the simulation performance of the proposed DT-based demonstrator is described. The system detects the activation/deactivation of faults affecting the individual electric motors and estimates the corresponding Failure Rate and Remaining Useful Lifetime of each EM.

The demonstrator front end is shown in Figure 4. The real-world simulated system is connected to the simulated cloud environment including the vehicle digital twin simulation model and the data analytics module. A set of switches activate/deactivate different faults affecting the different motors. The data analytics modules return the fault detection signals that are displayed on the set of green (fault-free) and red (faulty) lamp lights.

The Failure Rate and the Remaining Useful Lifetime computed by the data analytics module are shown in the graphs at the bottom of the demonstrator. Motors affected by more faults tends to have a RUL decreasing more rapidly than the fault-free EMs. In a similar manner, an EM affected by more faults tends to have a higher value of the Failure Rate (which reduces when the vehicle is not moving).

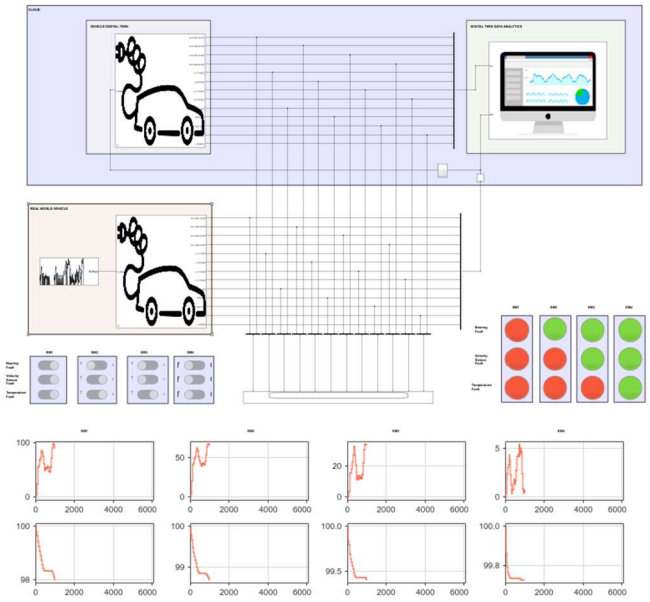

Fig. 4. Digital Twin demonstrator simulation system.

To validate the performance of the proposed DT-based fault monitoring approach, the demonstrator has been exploited to simulate different fault scenarios affecting the electric motors. In the following, one the different EMs is subject to different faults and demonstrate the effectiveness of the approach. Figure 5 shows the signals generated from the real-world EV EM model (red lines) and the related DT simulation system (blue lines).

The faults affecting the considered EM are: the bearing fault is activated at $t = 1116$ s, deactivated at $t = 2215$ and activated again at $t = 5222$ s; the speed sensor fault is activated between $t = 2215$ s and $t = 3369$ s, and activated again at $t = 5222$ s; the temperature fault is activated at $t = 3370$ s, deactivated at $t = 4417$ s, and activated again at $t = 5222$ s.

The performance of the proposed DT-based data-driven fault detection approach is shown in Figure 6, where the extracted feature signals (blue lines), the fault activation signals (red lines), the averaged feature values (yellow lines) and the fault alarm signals (purple lines) are shown for different motors. The ability of the proposed method to detect the activation and deactivation of faults is demonstrated, and detection delays relatively small.

The vibration fault signal change is detected with an averaged delay of 85 s, the speed sensor data is detected with an averaged delay of 76 s and the temperature fault with an averaged delay of 141 s.

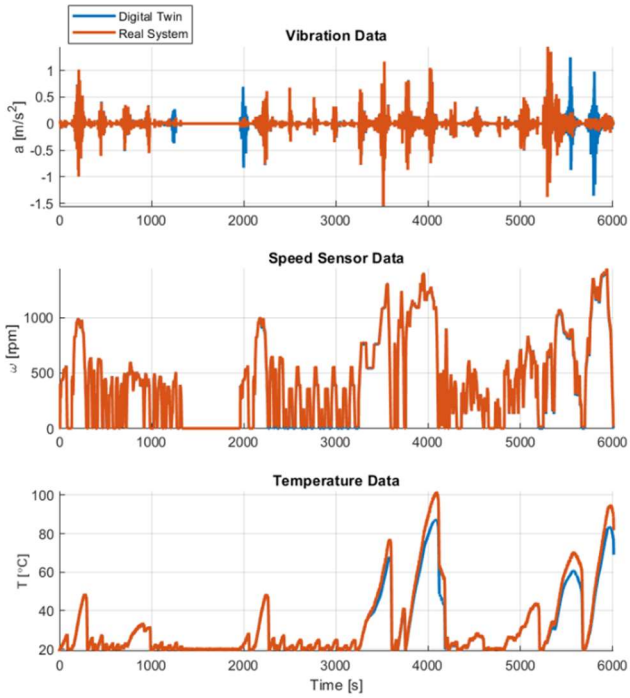


Fig. 5. Real-World model and Digital Twin signals

These detection intervals could be reduced by increasing the complexity of the selected data-driven algorithms (e.g., increasing the transmission rate or adjusting the average featured buffer size and update policy). Only a limited number of false alarms (each of limited duration) are detected relating to the bearing fault, around $t = 5700$ s, due to the change of dynamics that is not captured by the DT model and thus it is wrongly considered as a faulty condition. Finally, the estimated Failure Rate and the Remaining Useful Lifetime of the selected EM are shown in Figure 7.

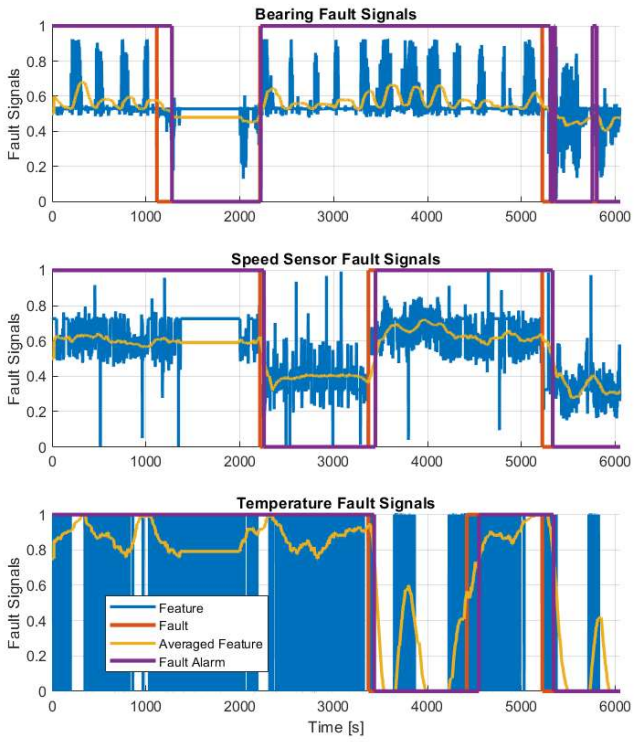


Fig. 6. Fault detection algorithms signals

The estimated FR of the EM tends to increase when more faults are detected on the different EM components, whereas it decreases when the EM operates in fault-free conditions. On the other hand, the slope of the trajectory shown in the lower plot of Figure 7 shows how the estimated RUL tends to decrease rapidly when more faults are detected and more slowly in fault-free conditions.

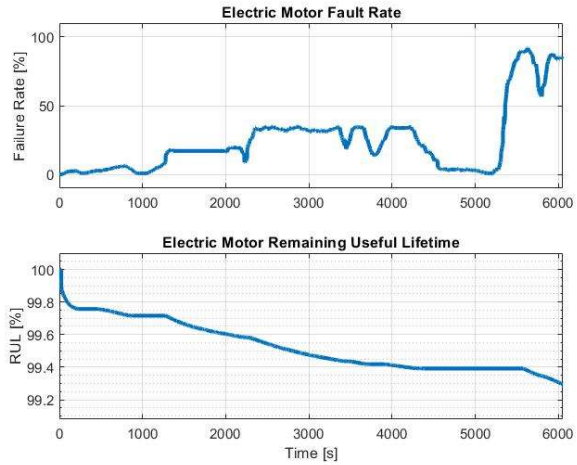


Fig. 7. State of Health monitoring algorithms signals

## VI. CONCLUSIONS

The application of Digital Twin technology to the State of Health monitoring problem of Electric Motors in Electric Vehicles has been proposed. Different data-driven Machine Learning methods, such as Neural Networks and Support Vector Classifier, were applied to detect faults, based on a comparison of real-world and virtual model signals. Furthermore, the features were exploited for estimating Failure Rate and Remaining Useful Lifetime of each Electric Motor. A set of simulation scenarios was considered for evaluating the performance of the system. Future research directions will consider the application of the proposed approach to other Electric Vehicle components involving more complex and interconnected subsystem dynamics.

## REFERENCES


[1] Shafto, M., Conroy, M., Doyle, R., Glaessgen, E., Kemp, C., LeMoigne, J., & Wang, L., "Modeling, simulation, information technology & processing roadmap.," National Aeronautics and Space Administration, 1-38, 2012.

[2] Lim, Kendrik Yan Hong, Pai Zheng, and Chun-Hsien Chen., ""A state-of-the-art survey of Digital Twin: techniques, engineering product lifecycle management and business innovation perspectives," *Journal of Intelligent Manufacturing,* vol. 31, no. 6, pp. 1313-1337, 2020.

[3] Wang, Z, "Digital Twin Technology," *Industry 4.0-Impact on Intelligent Logistics and Manufacturing;,* 2020..

[4] Grieves, M.; Vickers, J., Digital twin: Mitigating unpredictable, undesirable emergent behavior in complex systems, Springer, 2017.

[5] Hosamo, H. H., Svennevig, P. R., Svidt, K., Han, D., & Nielsen, H. K., "A Digital Twin predictive maintenance framework of air handling units based on automatic fault detection and diagnostics," *Energy and Buildings,* vol. 261, 2022.

[6] Lei, Y., Li, N., Guo, L., Li, N., Yan, T., & Lin, J., "Machinery health prognostics: A systematic review from data acquisition to RUL prediction," *Mechanical systems and signal processing ,* vol. 104, pp. 799-834, 2018.

[7] Lee, Seung Woo, and Hwa Ki Lee, "Reliability prediction system based on the failure rate model for electronic components," *Journal of mechanical Science and Technology,* vol. 22, no. 5, pp. 957-964, 2008.

[8] Samuel, S., Austin, L., & Morrey, D., "Automotive test drive cycles for emission measurement and real-world emission levels-a review," *roceedings of the Institution of Mechanical Engineers, Part D: Journal of Automobile Engineering,* vol. 216, no. 7, pp. 555-564, 2002.

[9] Cavanini, Luca, Gionata Cimini, and Gianluca Ippoliti., "Computationally efficient model predictive control for a class of linear parameter-varying systems," *IET Control Theory & Applications,* vol. 12, no. 10, pp. 1384-1392, 2018.

[10] Madhu, Remitha K., and Anna Mathew, "Matlab/simulink model of field oriented control of pmsm drive using space vectors," *International Journal of Advances in Engineering & Technology,* vol. 6, no. 3, p. 1355, 2013.

[11] Amin, F., Sulaiman, E. B., Utomo, W. M., Soomro, H. A., Jenal, M., & Kumar, R. , "Modelling and simulation of field oriented control based permanent magnet synchronous motor drive system," *Indonesian Journal of Electrical Engineering and Computer Science,* vol. 6, no. 2, pp. 387-395, 2017.

[12] Bourogaoui, M., H. Ben Attia Sethom, and I. Slama Belkhodja, "Speed/position sensor fault tolerant control in adjustable speed drives–A review," *Isa Transactions ,* vol. 64, pp. 269-284, 2016.

[13] Padeborn University, [Online]. Available: https://www.kaggle.com/datasets/wkirgsn/electric-motor-temperature.

[14] Cavanini, L., Cimini, G., Ferracuti, F., & Ippoliti, G., "Reference governor for switching converters with power factor correction," in *IEEE European Control Conference (ECC)* , 2021.

[15] [Online]. Available: https://engineering.case.edu/bearingdatacenter/download-data-file.

[16] Chow, M-Y., Robert N. Sharpe, and James C. Hung., "On the application and design of artificial neural networks for motor fault detection," *IEEE Transactions on industrial electronics,* vol. 40, no. 2, pp. 189-196, 1993.

[17] SAMANTA, BISWAJIT; AL-BALUSHI, K. R.; AL-ARAIMI, S. A., “Artificial neural networks and support vector machines with genetic algorithm for bearing fault detection,” *Engineering applications of artificial intelligence,* vol. 16, no. 7, pp. 657-665, 2003.

[18] Musavi, M. T., Ahmed, W., Chan, K. H., Faris, K. B., & Hummels, D. M., “On the training of radial basis function classifiers,” *Neural networks,* vol. 5, no. 4, pp. 595-603, 1992.

[19] Cavanini, L., Ferracuti, F., Longhi, S., & Monteriù, A., “Ls-svm for lpv-arx identification: Efficient online update by low-rank matrix approximation,” in *IEEE International conference on unmanned aircraft systems (ICUAS)*, 2020.

[20] Cavanini, L., Ferracuti, F., Longhi, S., Marchegiani, E., & Monteriù, A., “Sparse approximation of ls-svm for lpv-arx model identification: Application to a powertrain subsystem,” in *IEEE AEIT International Conference of Electrical and Electronic Technologies for Automotive (AEIT AUTOMOTIVE)*, 2020 .

[21] Aivaliotis, P., Georgoulias, K., Arkouli, Z., & Makris, S., “Methodology for enabling digital twin using advanced physics-based modelling in predictive maintenance,” *Procedia Cirp,* vol. 81, pp. 417-422, 2019.